Rubber-elastic behaviour of poly(vinyl chloride) craze during discontinuous fatigue crack growth

Y. Imai, T. Takase*, T. Ikeda and T. Ohno
Department of Mechanical Systems Engineering, Nagasaki University, Nagasaki 852, Japan
(Received 13 April 1994)

Deformation of crack-tip crazes was measured on poly(vinyl chloride) by the optical interference method when the fatigue crack grew discontinuously. The changes in the craze displacements and stresses during a crack growth retarded period were then analysed. With load repetition, crazes increase their size and deform rubber-elastically. Employing the inverse Langevin approximation, a model was proposed that attributes the increase of rubber-elastic extension to the increase of random links between tangled junctions of molecular chains in craze fibrils through disentanglement. The number of links was found to increase almost linearly with repetition. The model explains the change of craze stress–extension relation and also the difference of fracture-surface roughness.

(Keywords: poly(vinyl chloride); crack-tip craze; rubber-elastic behaviour)

INTRODUCTION

Fatigue cracks of some thermoplastics grow discontinuously depending on the intensity of loading, and arrest bands are observed on the fractured surface similar to the usual fatigue striations. Since the first observation of this type of growth, macroscopic variables such as band widths and retarded cycles have been studied and successfully related to the applied stress intensity range[1-3]. Recently, microscopic investigations were carried out in order to get a full understanding of the mechanism. Könczöl *et al.*[4] measured the deformation of crack-tip crazes of several polymers by interference optics and found the critical extension ratio of craze fibrils that should be reached when a crack jump occurs. They also imagine the damage mechanism as a disentanglement process.

In this paper, experiments and analyses supporting the above idea of a disentanglement process will be presented. The craze deformation during one fatigue cycle and the change of the craze stress–extension relation in the course of crack growth retarded duration (GRD) will be analysed employing a similar method of analysis as before[5]. Then, the craze fibrils will be shown to deform rubber-elastically with the load repetition. With the inverse Langevin approximation[6,7] being employed, the increase of craze extension is attributed to the increase of random links in a molecular chain of craze fibrils, that is, the decrease of physical entanglement of molecular chains. The result is very suggestive for the mechanism of the disentanglement process.

*To whom correspondence should be addressed

0032-3861/94/26/5678–07

EXPERIMENTAL METHOD AND ANALYSIS

Measurements were conducted on poly(vinyl chloride) (PVC) with a weight-average molecular weight of 30 000. The same loading apparatus as before[5] was installed on the microscope stage and CT specimens of $12 \times 12.5 \times 5\ mm^3$ were fatigued at the rate of 1/60 Hz. During the fatigue loading, the crack-tip region was observed from the direction normal to the crack face and interference patterns like that shown in *Figure 1* were recorded continuously on a VTR. The patterns were also photographed and analysed. The fringe order j can be converted into the deformed craze displacement 2δ using the wavelength L of the light and the refractive index μ of the craze as:

$$2\delta = jL/2\mu \tag{1}$$

Since the craze is very thin (usually less than several micrometres) compared to its length R, the deformation of the bulk region surrounding the craze can be well approximated by the Dugdale model. Assuming that the bulk material, $2g$ wide, deforms into a craze 2δ, on application of the craze stress $\sigma(r)$, the elastic displacement of the craze–bulk interface, $\delta(r)-g(r)$, may be expressed as[5]:

$$\delta(r)-g(r) = \frac{2(1-\nu^2)}{\pi E}\left((2\pi r)^{1/2}K_I - \int_0^R \sigma(s)\log\left|\frac{s^{1/2}+r^{1/2}}{s^{1/2}-r^{1/2}}\right| ds\right) \tag{2}$$

where K_I is the applied stress intensity factor, E and ν are the Young's modulus and Poisson's ratio of the bulk material, respectively, and r is measured from the craze tip. In the following, $E/(1-\nu^2)=2.5$ GPa was used.

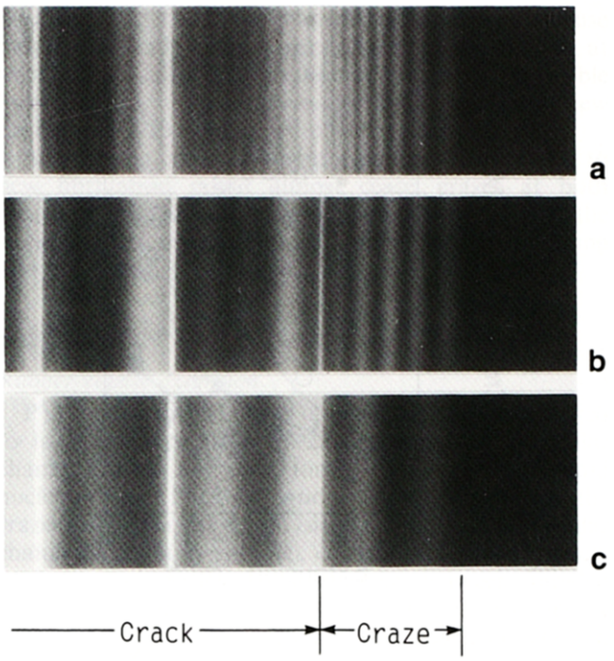

Figure 1 Change of interference fringe observed near the PVC fatigue crack tip: (a) $K_I = 0.35$ MPa m$^{1/2}$, (b) $K_I = 0.14$ MPa m$^{1/2}$, (c) $K_I = 0.02$ MPa m$^{1/2}$

Stress singularity at the craze tip can be eliminated by the condition:

$$K_I = (2/\pi)^{1/2} \int_0^R \frac{\sigma(s)}{s^{1/2}} ds \tag{3}$$

The refractive index of an extended craze was estimated from the Lorentz–Lorenz equation[8] with the bulk index μ_0 (= 1.56) and craze extension ratio λ as:

$$\frac{\mu^2 - 1}{\mu^2 + 2} = \left(\frac{\mu_0^2 - 1}{\mu_0^2 + 2}\right) \frac{1}{\lambda} \tag{4}$$

Permanent strain of the craze is obtained by inserting the index $\mu = 1.30$ (ref. 1) for the relaxed craze into equation (4) to be $\lambda_0 = 1.73$. Assuming that the craze strain at the minimum load falls to this relaxed level, as Könczöl *et al.* did[4], the craze original width $g(r)$ was estimated using the craze displacement at the minimum load around $K_I = 0.02$ MPa m$^{1/2}$.

The craze extension ratio is then estimated as:

$$\lambda = \delta / g \tag{5}$$

Solving equations (1) to (5) simultaneously with the applied stress intensity factor K_I and the measured fringe order j as a function of the distance from the craze tip, the craze stresses and extension ratios were obtained.

EXPERIMENTAL AND ANALYTICAL RESULTS

Craze growth

The interference patterns shown in *Figure 1* were obtained under the loading condition $K_I = 0.02$–0.35 MPa m$^{1/2}$, where the crack front jumped for 88 μm almost instantaneously in the course of loading after 1588 cycles retarded. Even while the crack growth was interrupted, the crack-tip craze increased its length, especially at the early stage of GRD as shown *Figure 2*. The observed lengths have a great scatter although the craze length was reported to have ΔK_I dependence[3]. Under about $\Delta K_I = 0.3$ MPa m$^{1/2}$, for example, 100 μm craze was measured as seen in *Figure 1*, although lengths of 20–30 μm were observed predominantly. These may be caused by the extremely slow repetition rate employed.

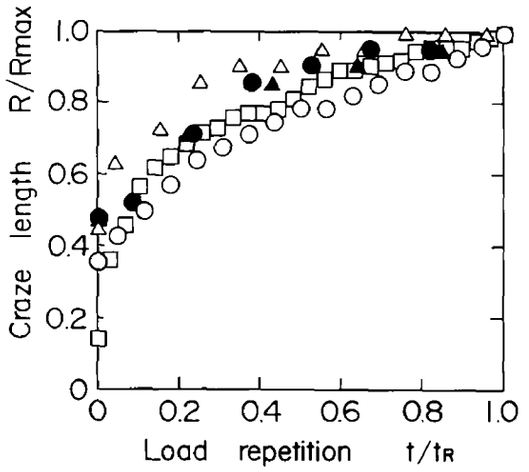

Figure 2 Growth of craze length during retarded duration t_R: (●) $K_I = 0.36$ MPa m$^{1/2}$, $t_R = 205$; (□) $K_I = 0.33$ MPa m$^{1/2}$, $t_R = 1588$; (○) $K_I = 0.32$ MPa m$^{1/2}$, $t_R = 1716$; (△) $K_I = 0.31$ MPa m$^{1/2}$, $t_R = 594$; (▲) $K_I = 0.29$ MPa m$^{1/2}$, $t_R = 1496$

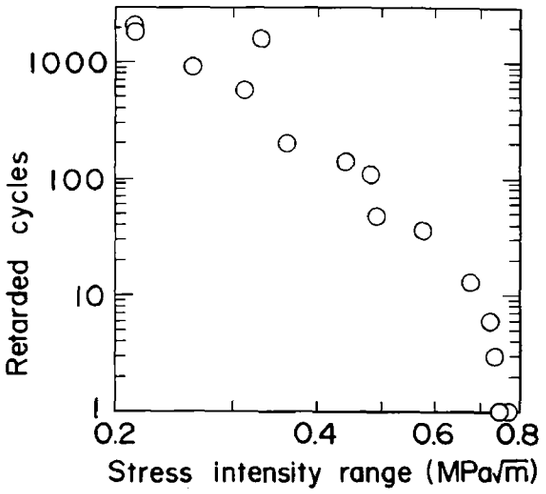

Figure 3 Stress intensity dependence of crack growth retarded duration t_R

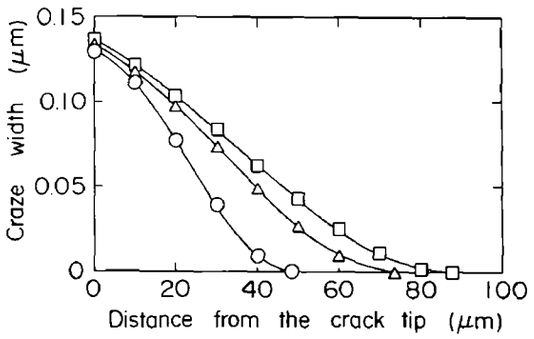

Figure 4 Growth of craze width during retarded duration: (○) $t/t_R = 0.10$; (△) $t/t_R = 0.48$; (□) $t/t_R = 0.97$; $t_R = 1588$

The GRD varied with the loading level as shown in *Figure 3*. The higher K_I, the shorter the GRD becomes until the crack finally grows every cycle.

Craze displacement and stress

The deformation of the craze shown in *Figure 1* was, at first, analysed at 10%, 48% and 97% of the GRD. *Figure 4* shows the craze original width distribution. Near the crack tip, the width did not increase so much after 10%. At other locations, however, new fibrillation widened the craze associated with lengthening. Craze widening as well as lengthening were intensive at the early stage of GRD.

Craze displacement at the maximum load is shown in *Figure 5*, being a similar distribution as the one obtained for continuously growing cracks. With repetition, the crack opening displacement became larger more or less proportionally to the increase of craze length, although the craze original width near the crack tip increased very little. This indicates that the craze strain near the crack tip increases with repetition.

The craze stress distributions are somewhat even except near the crack tip, as seen in *Figure 6*. The stress concentration at the crack tip appeared in the early stage gradually decreased with repetition. The longer craze gives the lower stress as expected by the Dugdale model and the lower stress will suppress new fibrillation at the craze–bulk interface, which may result in the saturation of craze widening as seen in *Figure 4*.

Stress–extension relation

The craze displacements and stresses at various load levels give the relation between the craze stress and the extension ratio as indicated by symbols in *Figure 7*, where the relations were estimated for the craze shown in *Figure 1* at positions 5 and 40 μm away from the crack tip. The n in the diagram will be discussed later.

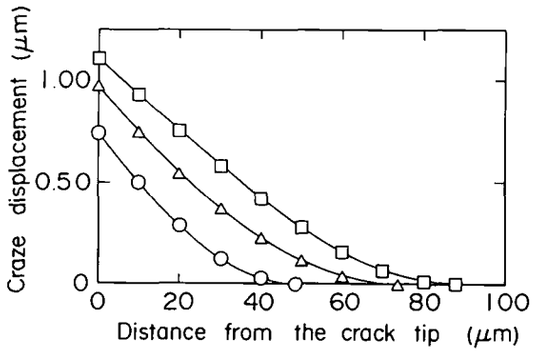

Figure 5 Craze displacements at the maximum load (symbols as for *Figure 4*)

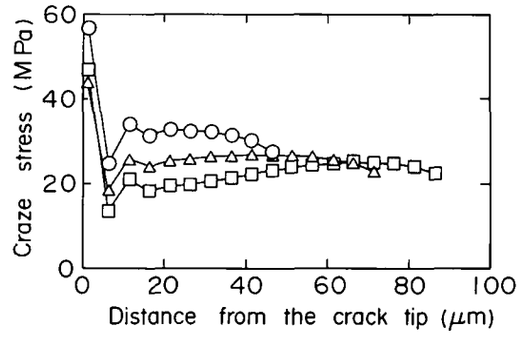

Figure 6 Nominal stress distributions at the maximum load, $K_I = 0.35$ MPa m$^{1/2}$ (symbols as for *Figure 4*)

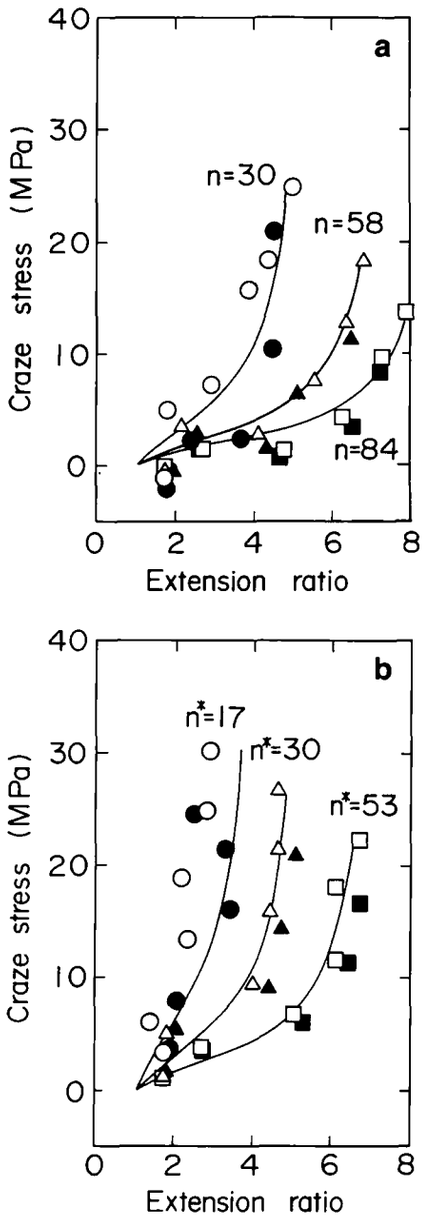

Figure 7 Stress vs. extension relation of craze fibrils measured in loading (open symbols) and unloading (full symbols) at (a) 5 μm and (b) 40 μm away from the crack tip (symbols as for *Figure 4*)

In the early stage of GRD, paths of loading (open symbols) and unloading (full symbols) did not coincide, showing hysteresis. As the load repetition proceeded, however, the craze gradually came to deform non-linear-elastically, that is, rubber-elastically, with diminishing hysteresis.

Comparing the relations of 10% life at these two locations also reveals the change of deformation pattern. The craze fibrils at 40 μm from the crack tip deformed fairly linearly in loading, probably because the craze was just fibrillated at 10% life as can be surmised from the craze with distribution in *Figure 4*. In contrast to this,

the craze fibrils at 5 μm deformed non-linearly because they had already been subject to the fatigue loading at least for 10% of GRD after the crack jump. Considerable hysteresis in unloading might be caused by new fibrillation at the peak load of this cycle.

At 97% life of GRD where widening of craze due to new fibrillation might almost cease, crazes at both locations changed to deform rubber-elastically and the stress–extension relation traced the same path in loading and unloading.

DISCUSSION

Rubber-elastic extension

PVC, consisting of linear molecular chains, is believed to form a bulky state by entanglement of molecular chains. Crazes are then formed through micro-void nucleation and fibril formation[9]. Now, assume that the craze fibrils consist of physically entangled molecular chains (N per unit volume), each of which has n freely jointed random links on average between tangled junctions. When the above random-coil network is subjected to a simple extension in the ratio λ, the required tensile force per unit unstrained area, σ, can be expressed from the inverse Langevin approximation[6,7] as:

$$\sigma=\frac{NkT}{3}n^{1/2}\left[\mathscr{L}^{-1}\left(\frac{\lambda}{n^{1/2}}\right)-\frac{1}{\lambda^{3/2}}\mathscr{L}^{-1}\left(\frac{1}{(\lambda n)^{1/2}}\right)\right] \quad (6)$$

where $\mathscr{L}^{-1}(\alpha)=\beta$ is the inverse Langevin function and $\alpha=\mathscr{L}(\beta)=\coth\beta-1/\beta$; k and T are the Boltzmann constant and the absolute temperature, respectively.

Larger number of random links gives larger extension for the same stress. Therefore, according to the inverse Langevin approximation, the increase of craze extension due to load repetition can be attributed to the increase of random links in molecular chains of craze fibrils. Furthermore, the increase of random links may be brought about through the disentanglement of molecular chains as schematically illustrated in *Figure 8*. In this case, however, it is to be noted that disentanglement reduces the number of network chains, N, provided that no chain scissions occur. Consequently, if we ignore the chain scissions and employ equation (6) for the craze extension, it is natural to use the restriction that the total number of links per unit volume of craze, nN, should be kept constant.

Now, let us see how equation (6) approximates the craze extension selectively near the crack tip where the craze original width changes very little with repetition, suitable for the application. The full curves in *Figure 7a* give the relation of equation (6) for the value of n labelled in the diagram and $NnkT/3=16$ MPa. Good approximation was obtained. Another example shown in *Figure 9a*, 3 μm away from the crack tip, also demonstrates that the measured extension is well represented by the rubber-elastic extension itself, although smaller n values are used compared to *Figure 7a*.

For a freshly fibrillated craze, on the other hand, the internal energy contribution[7] cannot be ignored any more. *Figure 9b* shows the case where GRD is quite short, 143 cycles, and the load repetition is limited. Measured extension ratio was fitted by adding the energy-based strain with the modulus of 50 MPa to the entropy-based one.

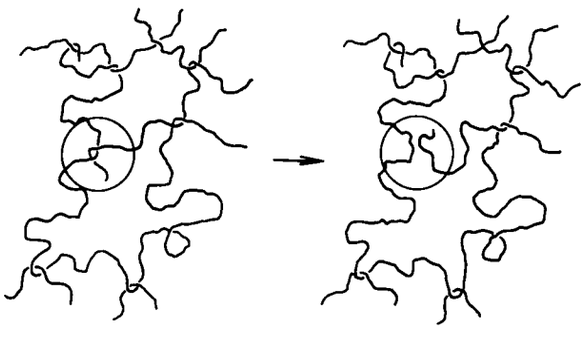

Figure 8 Disentanglement of molecular chains resulting in the increase of random links in a chain

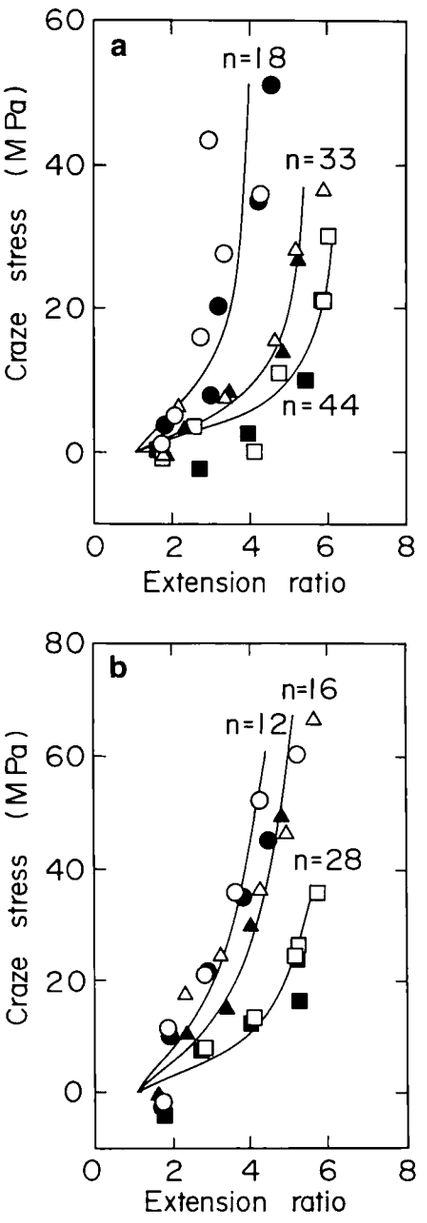

Figure 9 Approximation of craze stress vs. extension relation: (a) at 6% (○), 55% (△) and 95% (□) of 594 retarded cycles; (b) at 6% (○), 55% (△) and 95% (□) of 143 retarded cycles

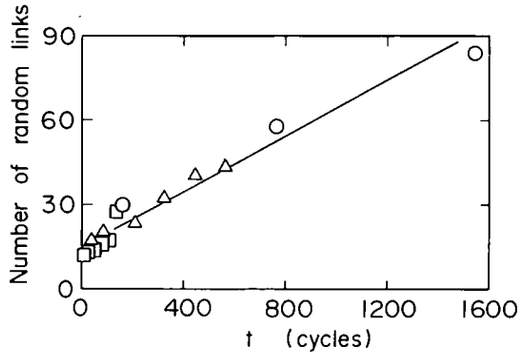

Figure 10 Increase of the number of random links in craze fibrils with load repetition: (○) $t_R = 1588$; (△) $t_R = 594$; (□) $t_R = 143$

Numbers of random links obtained near the crack tip are plotted in *Figure 10* against the load repetition after the crack jump. The number of links increases almost linearly with repetition at a rate possibly depending on the craze size and applied stress intensity factor.

Initial value of n just after the crack jump may be different with different craze condition because all parts of the craze fibrils near the crack tip were not freshly fibrillated at the moment of crack jump but some portion had already been fibrillated before the crack jump and subjected to loading in the previous GRD.

The linear increase of number of links, nonetheless, indicates that disentanglement occurs and the number of tangled junctions of molecular chains in a craze decreases at a constant rate with load repetition.

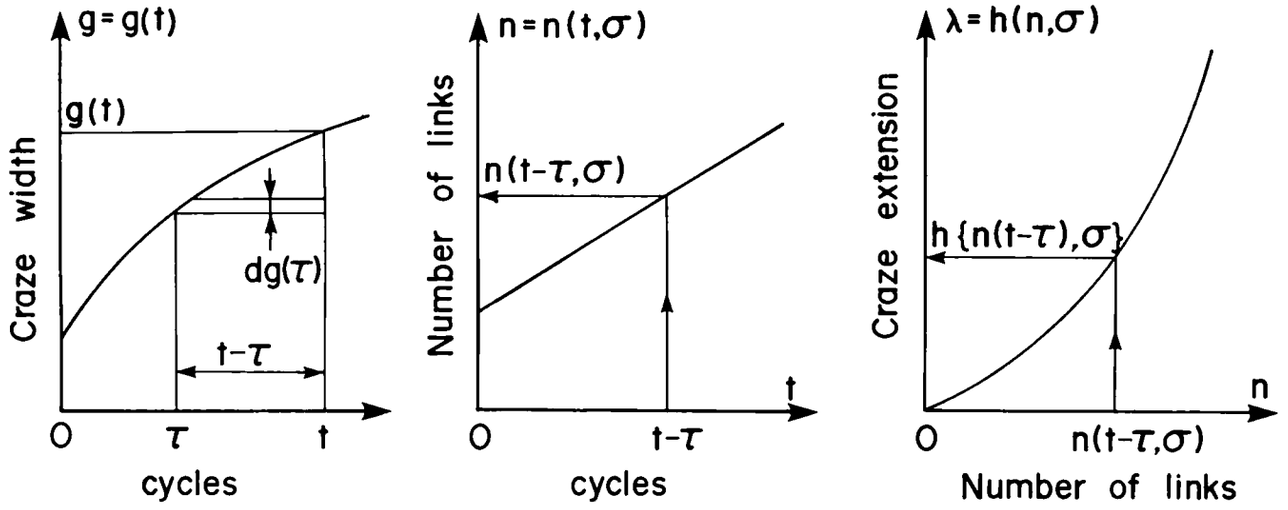

Figure 11 Estimating procedure of craze extension at any location

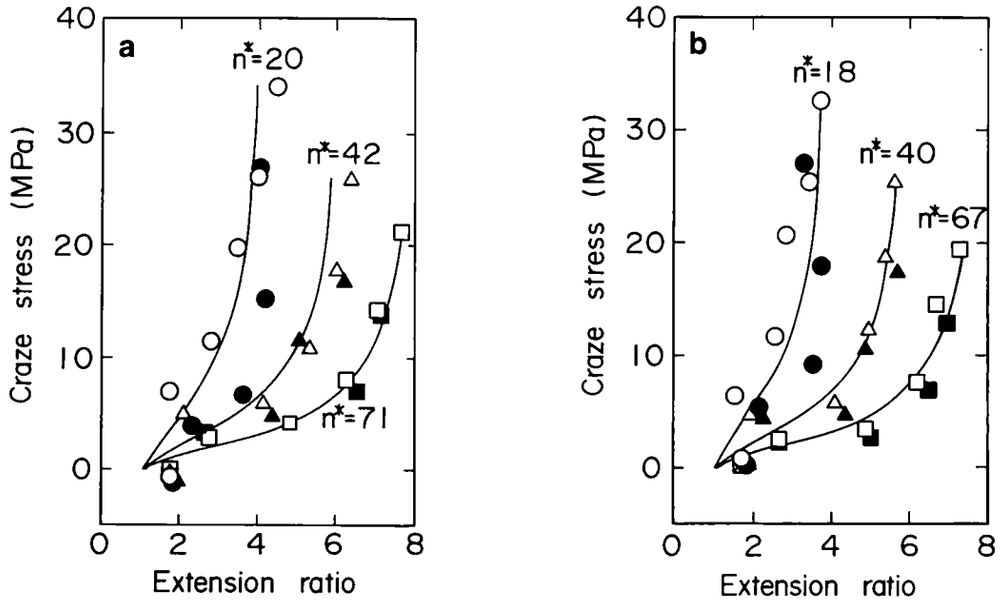

Figure 12 Stress vs. extension relations at (a) 10 μm and (b) 20 μm away from the crack tip (symbols as for *Figure 4*)

Craze extension

Near the crack tip, almost final width of the craze is rapidly attained in a very short duration after the crack jump and subsequent widening is little. At that location, the molecular network at any longitudinal position along the fibril is subjected to a similar number of repetitions and, hence, consists of a similar number of random links.

Far from the crack tip, on the other hand, the craze widens gradually by adding a new fibrillated part at the craze–bulk interface. Therefore, the molecular network at different longitudinal positions along the fibril is subjected to different numbers of repetitions. That is, the fibril has longitudinally varying number of random links. When this fibril is loaded, each molecular network in the fibril extends individually for the amount corresponding to its own number of links. The total extension may be the sum of such aligned extensions.

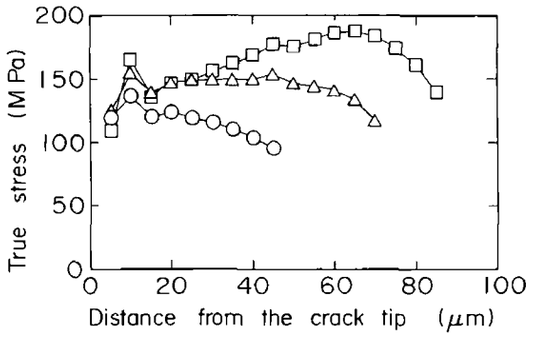

Figure 13 Distribution of true stress acting on the craze fibrils (symbols as for *Figure 4*)

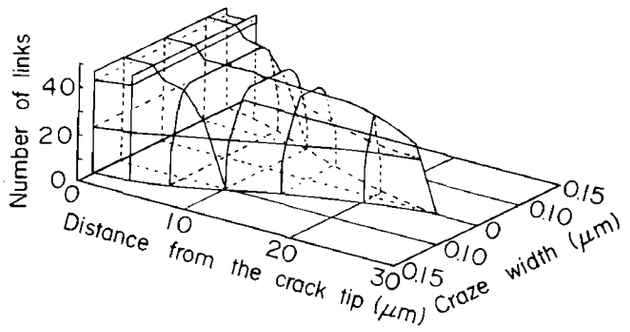

Figure 14 Density distribution of random links at 95% of 594 cycles GRD

Consequently, the craze extension at any location can be estimated as illustrated in *Figure 11*. At first, the craze widening history with the load cycles t is expressed as $g=g(t)$, the increase of number of links with cycles as $n=n(t,\sigma)$, and the inverse formula of equation (6), i.e. the extension is expressed as a function of number of links and stress, as $\lambda=h(n,\sigma)$. Then, the element $dg(\tau)$ fibrillated as $t=\tau$ will extend at $t=t$ subjected to the stress σ, to be:

$$h(n(t-\tau,\sigma),\sigma)\,dg(\tau)$$

Integrated between $\tau=t_0$ and $\tau=t$ and divided by the width at that moment, $g(t)$, the measured increment of total extension ratio, $\Delta\lambda_m$, will be obtained as:

$$\Delta\lambda_m=\left(\int_{t_0}^{t} h(n(t-\tau,\sigma),\sigma)\frac{dg}{d\tau}\,d\tau + h(n(t-t_0,\sigma),\sigma)g(t_0)\right)\Big/ g(t) \quad (7)$$

Using the craze width variation in *Figure 2* and increasing rate of number of links in *Figure 4*, stress–extension relations were theoretically estimated at locations 10, 20 and 40 μm from the crack tip at the cycles of 10%, 48% and 97% of GRD. In *Figure 12* and *Figure 7b*, the full curves are the estimations that approximate measured data expressed by symbols fairly well. The relations are also represented by nominal number of links, n^*.

Crack growth and roughness of fracture surface

The true stresses acting on the extended craze fibrils at the maximum load, obtained as the product of the nominal stress and extension ratio, are shown in *Figure 13*. The decrease of nominal stress with repetition as seen

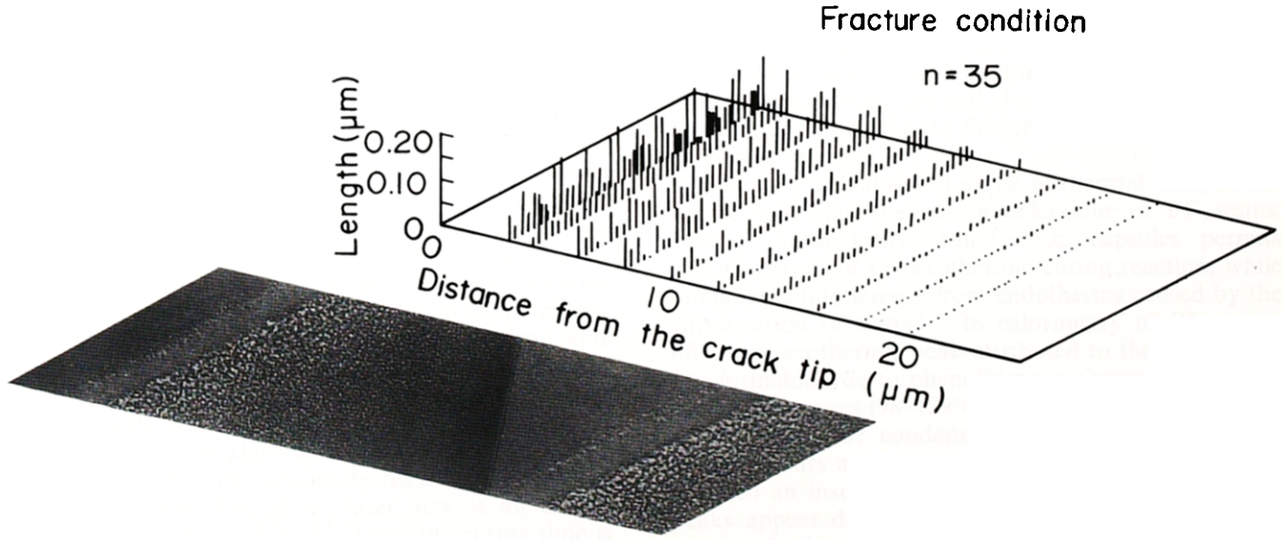

Figure 15 Computer simulation of fractured surface roughness and SEM micrograph showing the gradual change of roughness between adjacent crack arrest bands

in *Figure 6* was compensated by the increase of extension ratio. The true stress gradually increases with load repetition over the whole length of the craze, a favourable situation in preparation for the simultaneous breakdown of craze fibrils along a considerable length, that is, a crack jump.

Increasing of the number of links causes more extension of fibrils and higher true stress acting, which will enhance the possibility of fibril breakdown. *Figure 14* is an example of the three-dimensional diagram showing the density distribution of number of links at 95% of GRD (594 cycles) on the craze length vs. width plane. Near the crack tip, the density is evenly distributed along the craze width and, hence, any position along the craze fibril may become a breaking site. Apart from the crack tip, on the other hand, a high density is only achieved around the central portion of the craze width and the density gradually decreases towards the bulk interface. Therefore, only the central portion of the width may become the site at such lengthwise location.

The above consideration allows the computer simulation of length distribution of broken fibrils remaining on the fractured surface as shown in *Figure 15*, where fibril breakage was assumed to occur at random in the volume whose density of links exceeds 35. This simulation should be compared with a photograph of actual fractured surface between adjacent arrest bands shown in the same diagram. The rough surface in front of the arrest band and gradual decrease of roughness towards the next arrest band are well represented by the simulation.

CONCLUSIONS

From the measurement of the deformation of a crack-tip craze of PVC in the crack growth retarded duration, craze displacements and stresses were analysed. According to the craze growth in width and length with the load repetition, the nominal stresses acting on the craze–bulk interface gradually decrease, which suppresses new fibrillation and reduces craze growth. Craze fibrils deform rubber-elastically and the true stresses acting on fibrils increase over the craze length, which is favourable to simultaneous fibril breakdown.

Based on the inverse Langevin approximation, a model was proposed that relates the increase of rubber-elastic extension with the disentanglement of molecular chains in craze fibrils. The number of links increases almost linearly with repetition and, hence, it can be said that disentanglement of molecular chains occurs at a constant rate. The proposed model explains well the change of the stress–extension relation of crazes and also the change of roughness between two arrest bands on fractured surfaces.

REFERENCES

1 Mills, M. J. and Walker, N. *Polymer* 1976, **17**, 335
2 Hertzberg, R. W. and Manson, J. A. 'Fatigue of Engineering Plastics', Academic Press, New York, 1980, p. 160
3 Döll, W. 'Crazing in Polymers', Vol. 2, 'Advances in Polymer Science 91/92' (Ed. H. H. Kausch), Springer-Verlag, Berlin, 1990, p. 139
4 Könczöl, L., Döll, W. and Bevan, L. *Colloid Polym. Sci.* 1990, **268–9**, 814
5 Imai, Y., Takase, T. and Nakano, K. *J. Mater. Sci.* 1989, **24**, 3289
6 Treloar, L. R. G. 'The Physics of Rubber Elasticity', 3rd Edn, Oxford University Press, Oxford, 1975, p. 113
7 Ward, I. M. 'Mechanical Properties of Solid Polumers', 2nd Edn, Wiley, Chichester, 1983, p. 62
8 Brown, H. R. and Ward, I. M. *Polymer* 1973, **14**, 469
9 Kausch, H. H. 'Polymer Fracture', Springer-Verlag, Berlin, 1978, p. 272